THE JOURNAL OF PHYSICAL CHEMISTRY LETTERS
A JOURNAL OF THE AMERICAN CHEMICAL SOCIETY

pubs.acs.org/JPCL

Letter

Dynamic Role of the Intramolecular Hydrogen Bonding in the S_1 State Relaxation Dynamics Revealed by the Direct Measurement of the Mode-Dependent Internal Conversion Rate of 2-Chlorophenol and 2-Chlorothiophenol

Junggil Kim, Kyung Chul Woo, Minseok Kang, and Sang Kyu Kim*

Cite This: J. Phys. Chem. Lett. 2023, 14, 8428−8436

Read Online

ACCESS | Metrics & More | Article Recommendations | Supporting Information

ABSTRACT: The dynamic role of the intramolecular hydrogen bond in the S_1 relaxation of *cis*-2-chlorophenol (2-CP) or *cis*-2-chlorothiophenol (2-CTP) has been investigated in a state-specific manner. Whereas ultrafast internal conversion is dominant for 2-CP, the H-tunneling competes with internal conversion for 2-CTP even at the S_1 origin. The S_0-S_1 internal conversion rate of 2-CTP could be directly measured from the S_1 lifetimes of 2-CTP-d_1 (Cl-C_6H_4-SD) as the D-tunneling is kinetically blocked, allowing distinct estimations of tunneling and internal conversion rates with increasing the energy. The internal conversion rate of 2-CTP increases by two times at the out-of-plane torsional mode excitation, suggesting that the internal conversion is facilitated at the nonplanar geometry. It then sharply increases at ∼600 cm^{-1}, indicating that the S_1/S_0 conical intersection is readily accessible at the extended C−Cl bond length. The strength of the intramolecular hydrogen bond should be responsible for the distinct dynamic behaviors of 2-CP and 2-CTP.

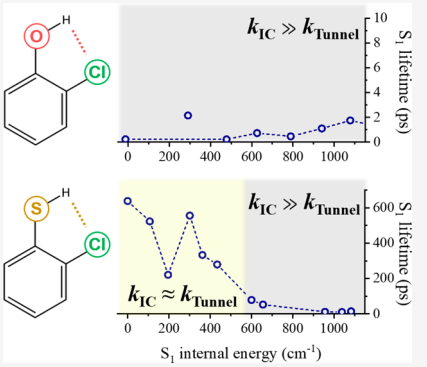

The $\pi\sigma^*$-mediated photochemistry of the heteroaromatic molecular system[1−5] has long been spotlighted not only because it gives the mechanistic clue for the ultrafast excited state relaxation of biological building blocks carrying the genetic code but also because it is extremely helpful to elucidate the nonadiabatic transition dynamics in the vicinity of the conical intersections.[6−10] The Born−Oppenheimer approximation breaks down when the conical intersections are encountered along the passage of the reactive flux, giving the nonstraightforward dynamic outputs of reaction rates, product yields, or branching ratios.[11−15] From the dynamic point of view, the $\pi\sigma^*$-mediated chemistry of the heteroaromatic system has provided the ideal model for investigating the predissociation dynamics (Herzberg type-I or -II)[16−18] and/or tunneling dynamics. In the predissociation event (e.g., the S−CH_3 bond dissociation of the S_1 thioanisole),[19−26] the reactive flux placed in the proximity of the conical intersection either nonadiabatically funnels through the narrowly defined conical intersection or sticks to the adiabatic potential energy surfaces to explore the phase space for riding on the minimum energy reaction path. For the tunneling case, the light atom (H or D) escapes from the S_1 potential well via tunneling through the barrier which is dynamically shaped by the upper-lying conical intersection.[27−30] Notably, the tunneling dynamics of the S_1 state has recently been thoroughly investigated in a state-specific way for a number of heteroaromatic molecular systems such as phenol,[27,31−34] substituted phenols,[35−44] *o*-cresol,[36,43] thiophenol,[45,46] 2-fluorothiophenol,[47,49,50] 2-methoxythiophenol,[48−50] or 2-chlorothiophenol.[47,49,50] It has been found that the tunneling dynamics in terms of the tunneling rate (also the energy disposal dynamics or nonadiabatic transition probability in some cases) are quite mode-dependent, and their qualitative behaviors could be rationalized from the dynamic shaping of the tunneling barrier by the upper-lying $S_1(\pi\pi^*)/S_2(\pi\sigma^*)$ conical intersection in many cases.[30,34,43,49]

Compared to the tunneling dynamics studies, the subject of the internal conversion of the $\pi\sigma^*$-mediated photochemistry of the heteroaromatic systems seems to be less explored especially as the presumably slower internal conversion process of the S_1 state of phenols or thiophenols is anticipated to be the minor channel.[33,51] However, as the system gets complexed through the functional group substitutions, the internal conversion process might become significant so that it could dominate over the tunneling reaction for some cases.[52] Among those $\pi\sigma^*$-mediated dynamics of the heteroaromatic systems, the S_1 state relaxation dynamics of 2-chlorophenol (2-CP) has been found to be quite distinct.[53,54] Most notably, Harris et al.[54] reported that the ultrafast internal conversion into the

Received: August 8, 2023
Accepted: September 12, 2023
Published: September 15, 2023

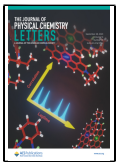

https://doi.org/10.1021/acs.jpclett.3c02208
J. Phys. Chem. Lett. 2023, 14, 8428−8436

vibrationally hot S_0 state should be largely responsible for the S_1 state relaxation of 2-CP. Photoexcitation in the spectral range of 266−193 nm gives rise to the product of HCl, Cl, or Cl*, presumably resulting from the unimolecular reaction of the vibrationally hot 2-CP in S_0. In contrast, H atom fragmentation turns out to be negligible. They suggested that the strong intramolecular hydrogen bonding (O−H···Cl) of 2-CP facilitates the S_0−S_1 internal conversion mediated by C−Cl bond elongation.

Herein, we have investigated the S_1 state dynamics of 2-CP using picosecond time-resolved pump−probe spectroscopy for the first state-specific lifetime measurements. The deuterated analogue of 2-CP-d_1 (where OH is substituted by OD) has also been studied for unraveling the possible kinetic isotope effect in the H(D) atom tunneling process. More importantly, we have explored the state-specific S_1 state dynamics of 2-chlorothiophenol (2-CTP) where the strength of the intramolecular hydrogen bonding (S−H···Cl) is expected to be weakened compared to the case of 2-CP. Quite interestingly, the H atom tunneling turns out to significantly contribute to the S_1 state relaxation of 2-CTP in the low internal energy region until it is overwhelmed by the rapid internal conversion process starting at ∼600 cm^{-1} above the S_1 zero-point energy level. Quite intriguingly, the internal conversion rate and the H atom tunneling rate of 2-CTP could be precisely determined by examining the S_1 lifetimes of 2-CTP-d_1 as the D atom tunneling from the latter is completely blocked (*vide infra*). The mode-specific internal conversion rate provides important mechanistic clues for the S_1−S_0 internal conversion process in terms of its reaction pathway and relevant energetic barrier. Competitive dynamics among tunneling and internal conversion of the S_1 2-CTP (or 2-CTP-d_1) has been discussed with the aid of the *ab initio* potential energy surfaces, giving deep insights into the role of the intramolecular hydrogen bonding in the S_1 state relaxation mechanism.

Resonance-enhanced two-photon ionization (R2PI) spectrum of 2-CP taken with the picosecond laser pulse (ΔE ∼ 20 cm^{-1}, Δt ∼ 1.7 ps) gives the Franck−Condon active S_1 vibronic bands as shown in Figure 1a. The spectral features of the *cis*-conformer could be mainly identified in the R2PI spectrum although the *trans*-conformer may be slightly populated (∼2%) in the jet-cooled molecular beam as the latter is estimated to be less stable than the former by ∼2.3 kcal/mol in the gas phase.[55−60] Although some vibronic bands could be well isolated in the frequency domain, most bands of *cis*-2-CP are found to be quite broad, implying that the associated lifetimes may be quite short. Indeed, the S_1 lifetime (τ) of the *cis*-2-CP is found to be shorter than a few picoseconds for all vibronic bands.[53,54] It should be noted, however, that the S_1 lifetime of the *cis*-2-CP is quite mode-dependent, and it is subject to further investigation (see Figure S6 of the Supporting Information). The picosecond time-resolved transient for each vibronic band shows the ultrafast single-exponential decay of which the subpicosecond time constant is beyond the current experimental temporal resolution (Figure S6). As a matter of fact, the S_1 origin of the *trans*-2-CP has been found to be located ∼190 cm^{-1} below that of the *cis*-2-CP.[53,61] In Figure 1d, the picosecond time-resolved transient gives τ = 1.1 ± 0.1 ns for the *trans*-conformer at the S_1 zero-point energy level (ZPL), which qualitatively is in accord with the previously reported fluorescence excitation spectroscopic study of the same system.[53] This lifetime of *trans*-2-CP is at least 3 orders of magnitude longer than the lifetime of the *cis*-2-CP, suggesting already that the intramolecular hydrogen bonding of the latter should make a huge difference in the S_1 state relaxation mechanism, and this is consistent with the previous other independent studies by Yamamoto et al.[53] and Harris et al.[54]

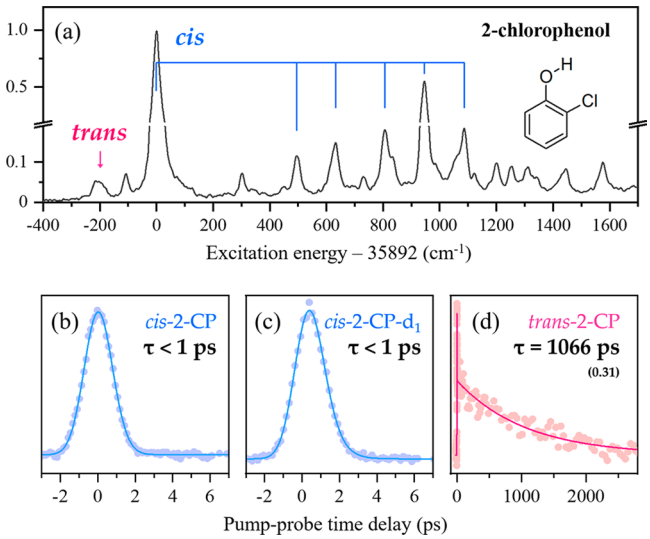

Figure 1. (a) Picosecond (1 + 1′) R2PI spectrum of 2-chlorophenol showing vibronic structures of the S_1−S_0 transition obtained at zero pump−probe time delay. The probe pulse wavelength was fixed at λ_{probe} = 285 nm. Parent ion transients and corresponding S_1 lifetimes of (b) *cis*-2-chlorophenol, (c) *cis*-2-chlorophenol-d_1, or (d) *trans*-2-chlorophenol at the zero-point energy level. The ion transient of *trans*-2-chlorophenol was fitted using biexponential function, and the fractional magnitude of the longer time component is shown in parentheses. Full experimental data are available in Figures S6 and S7 of the Supporting Information.

In order to make sure whether or not the H atom tunneling (which is the main relaxation pathway of the S_1 phenol) contributes to the S_1 state relaxation, we have carried out the picosecond pump−probe measurement for *cis*-2-CP-d_1 where the OH moiety is substituted by OD. In Figure 1c, it gives the same ultrashort S_1 lifetime with no kinetic isotope effect, strongly indicating that the H(D) atom tunneling dissociation from the OH(OD) moiety is little responsible for the S_1 state relaxation with nearly zero quantum yield. In order to further elaborate the H or D fragmentation mechanism of 2-CP-d_1, the relative yields of the H and D fragments have been estimated from their ion signals at the S_1 zero point energy level of the parent molecule (Figure S5 of the Supporting Information). Surprisingly, the H/D fragment yield ratio is estimated to be ∼3.8, which is nearly identical with the statistical ratio of 4, indicating that the H or D atom may be equally likely produced via the statistical unimolecular reaction of the vibrationally hot S_0 state which is prepared by the ultrafast S_0−S_1 internal conversion. Actually, this conforms to the S_1 lifetime measurements, as well as the absence of the kinetic isotope effect. According to the detailed study of 2-CP dynamics reported by Harris et al.,[54] the fast S_0−S_1 internal conversion which prevails even at the ZPL is ascribed to the significant effect of the strong (O−H(D)···Cl) intramolecular hydrogen bonding on the electronic configurations of the $\pi\sigma_{CCl}$* state especially with respect to the C−Cl bond extension coordinate. Namely, the adiabatic S_1 state (the first excited singlet state) becomes unbound due to the electronic configuration effect of the intramolecular hydrogen bonding

https://doi.org/10.1021/acs.jpclett.3c02208
J. Phys. Chem. Lett. 2023, 14, 8428−8436

when it is relaxed along the C−Cl bond extension coordinate, accelerating the eventual S_0−S_1 internal conversion.

The distinct dynamic behavior of the S_1 2-CP from many other different substituted phenols triggers the issue of the dynamic role of the intramolecular hydrogen bonding in the excited state relaxation, giving the important implications in the fast relaxation of the biological building blocks under various circumstances such as the localization of the hydrogen bonding in the hydrophobic environment, for instance.[62,63] For further investigation of this issue, we have tackled the S_1 state dynamics of 2-CTP and 2-CTP-d_1. In these systems, the strength of the S−H(D)···Cl intramolecular hydrogen bonding is expected to be weakened compared to the case of 2-CP due to the less electronegative nature of sulfur compared to oxygen. The R2PI spectra of 2-CTP and 2-CTP-d_1 taken with the picosecond laser pulse show the well-resolved S_1 vibronic bands which are totally attributed to the *cis*-conformer, Figure 2.[47] The S_1 lifetime, from the picosecond time-resolved parent ion transient, gives $\tau \sim 227 \pm 3$ or 638 ± 13 ps for the ZPL of 2-CTP or 2-CTP-d_1, respectively.[49,64] The first impressive finding would be that the H atom tunneling reaction does take place in these systems with a non-negligible quantum yield, and this is quite different from the case of 2-CP or 2-CP-d_1. It indicates that the H atom tunneling reaction should be less blocked in 2-CTP plausibly due to the weakened intramolecular hydrogen bonding. The second remarkable finding is that the H/D kinetic isotope effect of 2-CTP and 2-CTP-d_1 in terms of its S_1 lifetime is merely ~2.8 which is extremely small if the S_1 lifetime is mainly attributed to the H(D) atom tunneling reaction. Namely, it is far less than the kinetic isotope effect of ~23 or ~14 which had been found for 2-fluorothiophenol or 2-methoxythiophenol, respectively.[50] The tiny kinetic isotope effect of 2-CTP and 2-CTP-d_1 then strongly suggests that the contribution of the H atom tunneling dissociation to the S_1 state relaxation may not be large enough to account for the whole relaxation process. Instead, the concomitant S_0−S_1 internal conversion may kinetically compete even at the ZPL. Intriguingly, the S_1 lifetime of 2-CTP and 2-CTP-d_1 decreases very rapidly with the increase of the internal energy. That is, the lifetime of ~227 or ~638 ps of the respective 2-CTP or 2-CTP-d_1 at the ZPL falls down to converge into the time constant of ~60 ps at the internal energy of ~600 cm^{-1}. And then it further decreases to the subpicosecond lifetime at the internal energy of ~900 cm^{-1}. This rapid change of the S_1 lifetime as well as that of the kinetic isotope effect should reflect the unusual dynamic behavior of the S_0−S_1 internal conversion in the narrow energy region (*vide infra*).

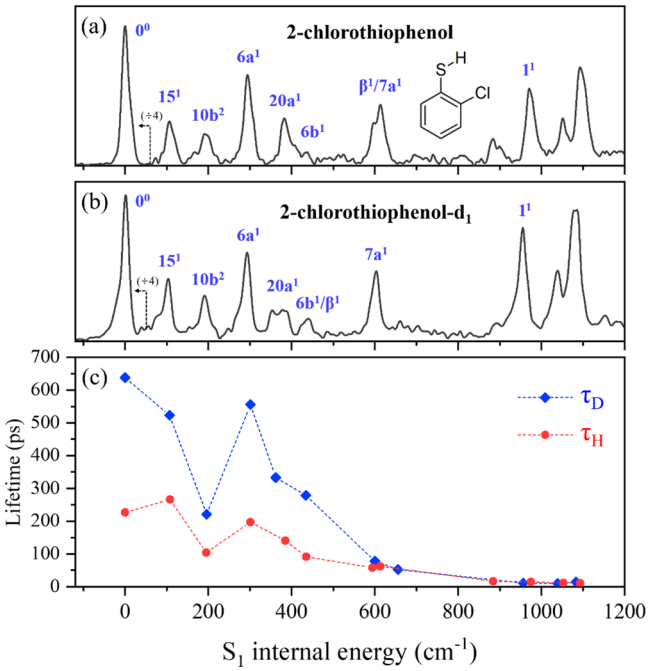

Figure 2. Picosecond R2PI spectra of (a) 2-chlorothiophenol and (b) 2-chlorothiophenol-d_1 obtained at zero pump−probe time delay. The probe pulse wavelength was fixed at λ_{probe} = 290 nm. Assignments and notations of vibrational normal modes have been adapted from refs 47 and 49. (c) S_1 lifetimes of 2-chlorothiophenol (τ_H, red circle symbols) and 2-chlorothiophenol-d_1 (τ_D, blue diamond symbols) obtained by fitting the parent ion transients using exponential decay molecular response functions. Full experimental data are available in Figure S8 of the Supporting Information.

The measured S_1 lifetime of 2-CTP ($\tau_H = k_H^{-1}$) or 2-CTP-d_1 ($\tau_D = k_D^{-1}$) represents the kinetic sum of its tunneling rate of k_H^T or k_D^T and the internal conversion rate (k_{IC}) as follows:

$$k_H = k_H^T + k_{IC} \tag{1}$$

$$k_D = k_D^T + k_{IC} \tag{2}$$

$$\frac{k_H}{k_D} = \frac{k_H^T + k_{IC}}{k_D^T + k_{IC}} \approx \begin{cases} \dfrac{k_H^T}{k_D^T} & (k_H^T > k_D^T \gg k_{IC}) \\ 1 & (k_{IC} \gg k_H^T > k_D^T) \end{cases} \tag{3}$$

Here, the internal conversion rate is taken to be the same for 2-CTP and 2-CTP-d_1, which seems to be a fairly good assumption as the S_0−S_1 coupling matrix elements as well as the density of states of two isotopologues are not anticipated to be largely changed by the subtle SH/SD substitution. Obviously, the convergence of the kinetic isotope effect into the unity (at ~600 cm^{-1}) is the consequence from the relation of $k_{IC} \gg k_H^T > k_D^T$, and completely explainable by the rapid increase of the internal conversion rate with the increase of the S_1 internal energy. In the low internal energy region, however, the H atom tunneling should compete with the internal conversion. In particular, the experimental finding that the apparent kinetic isotope effect of the S_1 lifetime ($k_H/k_D \sim 2.8$) is unusually small may suggest that the internal conversion rate is comparable with the tunneling rate in the low S_1 internal energy region. Namely, if the kinetic isotope effect of the pure tunneling reaction (k_H^T/k_D^T) is arbitrarily chosen to be ~20 according to our previous study,[50] then k_{IC} should be $\sim 1.4 \times 10^9$ s^{-1} ($\tau \sim 710$ ps) according to the above equation. This in turn gives the estimation of $k_H^T \sim 3.1 \times 10^9$ s^{-1} ($\tau \sim 330$ ps) and $k_D^T \sim 0.15 \times 10^9$ s^{-1} ($\tau \sim 6.51$ ns) at the ZPL. Though these absolute values of the kinetic rates may be less reliable, this estimation indicates that the internal conversion and H atom tunneling reactions are quite competitive for 2-CTP. On the other hand, as k_{IC} is much larger than k_D^T by an order of magnitude, the internal conversion is most likely to be totally responsible for the S_1 state relaxation of 2-CTP-d_1 because the D atom tunneling is kinetically much unfavorable. This strongly suggests that the S_0−S_1 internal conversion rate of 2-CTP (as well as 2-CTP-d_1) could be referred from the S_1 lifetime of 2-CTP-d_1 according to the kinetic equation (

https://doi.org/10.1021/acs.jpclett.3c02208
J. Phys. Chem. Lett. 2023, 14, 8428−8436

$k_D \cong k_{IC}$). It is quite intriguing to note that the internal conversion rate could be directly estimated in the mode-specific way by effectively blocking the otherwise competitive tunneling pathway of 2-CTP-d_1.[52] This makes it possible that the internal conversion rate (k_{IC}) and the H atom tunneling rate (k_H^T) could be separately extracted from the S_1 state lifetime of 2-CTP (k_H).

Kinetic competition between the S_0−S_1 internal conversion and H atom tunneling reaction in the S_1 state of 2-CTP derived from eqs 1−3 is illustrated in Figure 3. In the low S_1

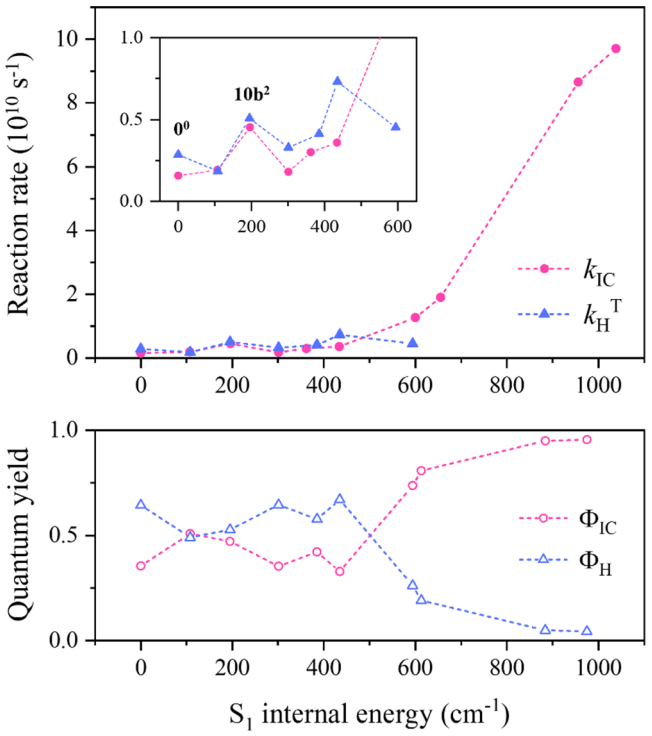

Figure 3. (Upper panel) Estimated reaction rates of the S_0−S_1 internal conversion (k_{IC}, red circles) and H atom tunneling (k_H^T, blue triangles) processes in the S_1 state of 2-chlorothiophenol as a function of the S_1 internal energy, derived from eqs 1−3 in the main text. Inset: Enlarged plot of the rates at the low S_1 internal energy region. (Lower panel) Quantum yields of two reaction channels obtained from the equations, $\Phi_{IC} = k_{IC}/(k_{IC} + k_H^T)$ and $\Phi_H = k_H^T/(k_{IC} + k_H^T)$. H atom tunneling rates above the S_1 internal energy of 600 cm^{-1} are assumed to remain constant.

internal energy range below ~400 cm^{-1}, k_{IC} and k_H^T are found to be quite comparable to give a relative quantum yield of ~0.5 for either the internal conversion or the H atom tunneling. The H atom tunneling rate of 2-CTP exhibits the strong mode-dependent behavior, giving the 2-fold increase of the tunneling rate upon the out-of-plane 10b^2 mode excitation to give $k_H^T \sim 5.1 \times 10^9$ s^{-1} compared to $k_H^T \sim 2.8 \times 10^9$ s^{-1} at ZPL. The abrupt increase of the tunneling rate had also been observed for 2-fluorothiophenol or 2-methoxythiophenol,[49,50] and it was nicely rationalized by the significant lowering of the adiabatic H atom tunneling barrier with respect to the C−C−S−H dihedral out-of-plane torsional coordinate.[50,65,66] Remarkably, the S_0−S_1 internal conversion rate is also found to have the substantial mode-dependent behavior, giving $k_{IC} \sim 4.5 \times 10^9$ s^{-1} at the 10b^2 mode excitation which is ~3-fold larger than $k_{IC} \sim 1.6 \times 10^9$ s^{-1} measured at ZPL. This indicates that the delocalization of the reactive flux along the nonplanar geometries should facilitate the internal conversion process of which the initial path involves the C−Cl bond extension (*vide infra*).

The dramatic increase of k_{IC} starting from the S_1 internal energy of ~600 cm^{-1} is obviously very different from the dynamic behavior of the H atom tunneling rate which converges and thereafter remains constant with the increase of the internal energy as the preceding intramolecular vibrational energy redistribution (IVR) is accompanied in the bound S_1 state.[33,50] As the S_1 internal energy increases more, the internal conversion becomes much faster than the tunneling reaction by more than 10-fold, giving nearly unity for the internal conversion quantum yield ($\Phi_{IC} \approx 1$). The sharp increase of k_{IC} has rarely been observed as one does not expect a sudden increase of neither the S_0-S_1 coupling strength nor that of the S_0 density of states in the corresponding very narrow energy range. Therefore, this indicates that the internal conversion may be facilitated by the access of the reactive flux above the adiabatic barrier (of ~600 cm^{-1}) which results from the $S_1(\pi\pi^*)/S_2(\pi\sigma_{CCl}^*)$ conical intersection encountered along the C−Cl bond extension coordinate. Once the reactive flux overcomes the barrier, it may reach the S_0/S_1 conical intersection through the repulsive potential energy surface in the later stage of reaction (*vide infra*). It is interesting to note that it had been suggested that the sharp increase of the internal conversion rate could be correlated to the barrier present along the ultrafast S_0−S_1 internal conversion pathway of the cytosine derivatives.[67,68]

For a comparison of the internal conversion mechanisms of 2-CP and 2-CTP, the adiabatic potential energy curves have been calculated for the S_1 states of those systems along the C−Cl bond extension coordinate. Interestingly, the minimum energy geometry optimized for the S_1 state using the density functional theory (DFT) or second-order approximate coupled cluster method (RICC2) adopts the nonplanar structure with the elongated C−Cl bond length for both molecules, suggesting that the S_1 state may be already quasi-bound in nature with respect to the C−Cl bond extension coordinate (Figure S4 of the Supporting Information). For unraveling the internal conversion pathway in a more sophisticated way, the single point CASPT2 calculations have been carried out at the DFT optimized S_1 geometries along the C−Cl bond extension coordinate with or without the C_s symmetry constraint, as shown in Figure 4. This two-step calculation method is almost same as one employed in ref 54. for the monosubstituted chlorophenol isomers. The resultant S_1 adiabatic potential energy curves with and without the C_s symmetry constraint converge at the large C−Cl bond distances for both 2-CP and 2-CTP to cross with the diabatic S_0 states leading to the internal conversion, although the detailed potential energy surfaces are quite distinct for two species. Namely, the S_1 potential energy curve of the planar geometry (with the C_s symmetry constraint) intersects with that of the nonplanar geometry (without the C_s symmetry constraint) with a shallow barrier of ~0.15 eV along the C−Cl bond extension coordinate for 2-CP whereas their intersection is predicted to be located a bit higher to give the barrier height of ~0.40 eV for 2-CTP. These adiabatic barriers are the consequences from avoided-crossings under the $S_1(\pi\pi^*)/S_2(\pi\sigma_{CCl}^*)$ conical intersection. Although absolute values of energetics associated with the adiabatic potential energy surfaces for both 2-CP and 2-CTP are subject to the further refinements, these potential energy schemes rationalize the experimental finding that the internal

https://doi.org/10.1021/acs.jpclett.3c02208
J. Phys. Chem. Lett. 2023, 14, 8428−8436

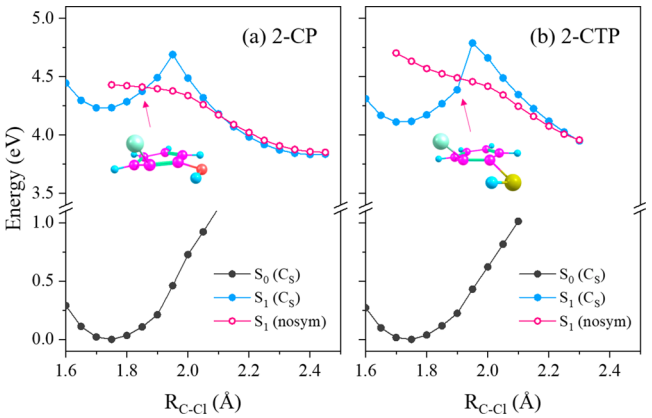

Figure 4. Relaxed potential energy curves for the S_0 (black filled circles) and S_1 states of (a) 2-chlorophenol and (b) 2-chlorothiophenol along the C−Cl bond extension coordinate with the C_s symmetry constraint (blue filled symbols) or no symmetry restriction (red open symbols). The molecular geometries at which two adiabatic S_1 curves cross near the Franck−Condon region are depicted. Color scheme for atoms: carbon, purple; hydrogen, blue; oxygen, red; sulfur, yellow; chlorine, green.

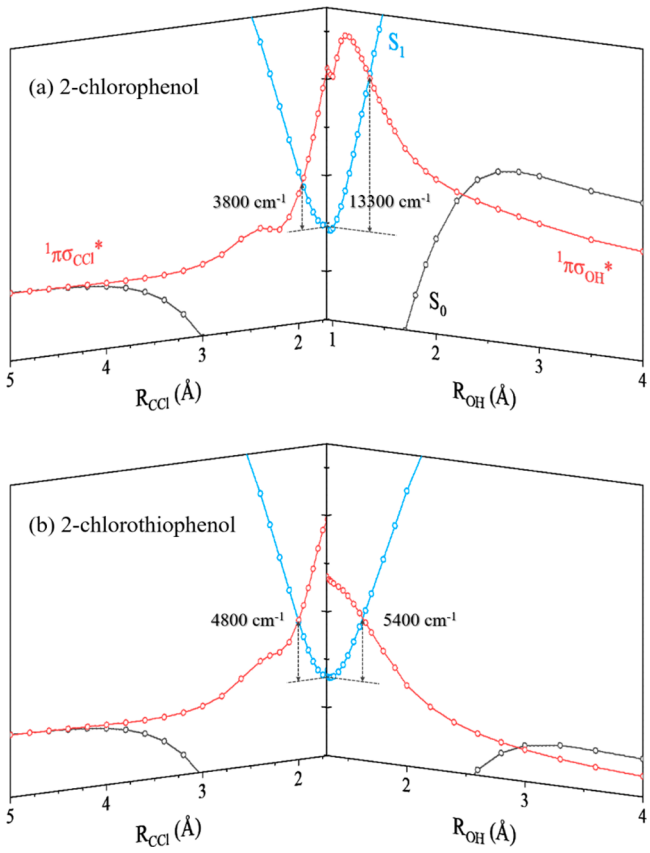

Figure 5. Schematic rigid-body scanned potential energy curves for the S_0 (black), S_1 ($\pi\pi^*$, blue), and S_2 ($\pi\sigma^*$, red) states of (a) 2-chlorophenol and (b) 2-chlorothiophenol along the C−Cl bond (left panel) or the O−H bond (right panel) extension coordinate. The molecular geometry is kept fixed at the S_0 equilibrium geometry with C_s symmetry, except the O−H or C−Cl bond length. Relative potential energies on the vertical z-axis are given in 0.5 eV per each tick.

conversion rate is already fast and dominant at the S_1 ZPL for 2-CP whereas it is comparable with the H atom tunneling until it rapidly increases to be dominant above the onset of ∼600 cm^{-1} for 2-CTP. The aforementioned large increase of the internal conversion rate of 2-CTP upon the $10b^2$ mode excitation (Figure 3) is also well rationalized as the reactive flux spread along the out-of-plane coordinate may be favored into the relaxation on the nonplanar adiabatic S_1 potential energy surface extended along the C−Cl bond stretching coordinate. The multidimensional potential energy surfaces calculations regarding the internal conversion process as well as tunneling reaction would be quite desirable for unraveling the mechanism of the whole S_1 state relaxation pathway.

In the previous individual reports by Yamamoto et al.[53] and Harris et al.,[54] it has been claimed that the strong intramolecular hydrogen bonding of 2-CP should be responsible for the stabilization (or equivalently lowering) of the $\pi\sigma_{CCl}$* state where the σ_{CCl}* is the antibonding orbital along the C−Cl bond elongation coordinate. The otherwise slow internal conversion ($\tau \sim 10$ ns for the S_1 phenol,[69,70] for instance) then becomes 4 orders of magnitude faster ($\tau < 1$ ps), giving the major relaxation pathway for the S_1 state decay of 2-CP. Rigid-scanned potential energy surfaces in Figure 5a show that the reaction barrier height of 13 300 cm^{-1} is required for the H atom tunneling along the O−H bond extension coordinate, which is extremely unfavorable compared to the internal conversion in the S_1 state of 2-CP. Quite interestingly, it has been newly found here that the internal conversion rate of 2-CTP has been substantially slowed compared to that of 2-CP in the low S_1 excess energy region, and it is attributed to the increase of the adiabatic barrier height along the internal conversion path leading to the S_0/S_1 conical intersection, Figures 4 and 5. In addition, the H atom tunneling from the SH moiety is greatly facilitated for 2-CTP as the corresponding tunneling barrier has been substantially lowered compared to that for the H atom tunneling from the OH moiety of 2-CP. Although absolute values of the barrier heights are likely to be overestimated, the overall potential energy surfaces depicted in Figure 5 give quite reasonable explanations of the experimental results. Accordingly, the relatively slow internal conversion in the S_1 low internal energy region of 2-CTP compared with that of 2-CP seems to originate from the relatively weaker intramolecular hydrogen bonding of the former compared to the latter. Namely, the stabilization of the $\pi\sigma_{CCl}$* state by the intramolecular hydrogen bonding is less effective in the 2-CTP compared to that in the 2-CP.

As a matter of fact, ultrafast internal conversion has rarely been reported in the heteroaromatic molecular systems of phenol or thiophenol derivatives. Although S_1 state of the monosubstituted chlorobenzene had been reported to undergo the internal conversion with the similar mechanism through the S_0/S_1 conical intersection developed along the C−Cl extension coordinate, its time constant remains at around the nanosecond time range.[71−75] The similar situation has also been found for other heteroaromatic systems with no intramolecular hydrogen bonding such as *trans*-2-chlorophenol or 3-chlorophenol. Even for 2-fluorophenol[37,54,76,77] or 2-fluorothiophenol[47,49,50] where the relatively weak intramolecular hydrogen bonding exists,[78−83] the ultrafast internal conversion such as found in the low S_1 internal energy region of 2-CP and 2-CTP could not be observed. It is intriguing to note, on the other hand, that the S_1 vibronic states of 2-chlororesorcinol (Figure S3 of the Supporting Information), 2-bromophenol,[53] or 2-bromothiophenol[84,85] are reported to be

https://doi.org/10.1021/acs.jpclett.3c02208
J. Phys. Chem. Lett. 2023, 14, 8428−8436

quite diffuse in the S_1-S_0 transition spectra due to the homogeneous lifetime broadening effect. The strong intramolecular hydrogen bonding of those systems may be responsible for the S_1 state's ultrafast relaxations via the ultrafast internal conversion process plausibly activated along the carbon−halogen bond extension coordinate. Phenomenal observation found here for 2-CP or 2-CTP in terms of the dynamic behavior of the S_1 state relaxation process is indeed quite intriguing, as the intramolecular hydrogen bonding seems to facilitate the otherwise slow internal conversion process. Chemistry of the vibrationally hot S_0 state of 2-CP or 2-CTP after the fast internal conversion is beyond our scope at the present time though the photochemical studies of such species in the matrix environment imply the existence of many interesting chemical changes into various products.[58,86]

In conclusion, the real-time S_1 state relaxation dynamics of 2-chlorophenol and 2-chlorothiophenol have been investigated here using narrow-band picosecond time-resolved pump−probe spectroscopy. The rapid S_0-S_1 internal conversion is largely responsible for the subpicosecond S_1 state lifetime of the *cis*-conformer of 2-chlorophenol, corroborating the previous findings by Yamamoto et al. and Harris et al. that the intramolecular hydrogen bonding facilitates the internal conversion activated by the C−Cl bond coordinate.[53,54] For 2-chlorothiophenol, on the other hand, it has been found that the internal conversion is significantly slowed in the low S_1 internal energy region compared to the case of 2-chlorophenol, allowing for the H atom tunneling reaction to compete with the internal conversion before the S_1 state relaxation is dominated by the internal conversion starting at ∼600 cm^{-1} above the S_1 zero-point energy level. The mode-dependent internal conversion rate of 2-chlorothiophenol could be directly estimated from the S_1 lifetimes of 2-chlorothiophenol-d_1 as the otherwise competing D atom tunneling reaction (from the SD moiety) is kinetically unfavorable. This makes it possible to extract the contribution of the H atom tunneling and that of the internal conversion to the S_1-state relaxation completely in a separate manner. Strong mode-dependent behavior of the internal conversion rate followed by the sharp increase in the narrow internal energy range provides the very important dynamic aspect of the internal conversion mechanism, where the reactive flux should experience the adiabatic barrier set by the $S_1(\pi\pi^*)/S_2(\pi\sigma_{CCl}^*)$ conical intersection along the C−Cl extension coordinate before it reaches the internal-conversion funnel of the S_0/S_1 conical intersection. The intramolecular hydrogen bonding of 2-chlorothiophenol substantially weakened compared to that of 2-chlorophenol is most likely responsible for the slower internal conversion of the former compared to the latter, which is also supported by the *ab initio* potential energy surface calculations. The dynamic role of intramolecular hydrogen bonding in expediting the internal conversion of the electronically excited state seems to be a fascinating subject. Our complete experimental investigations combined with *ab initio* calculations give the unprecedented deep insights into the role of the intramolecular hydrogen bonding in the excited state relaxation dynamics of the $\pi\sigma^*$-mediated systems. The conceptual advance obtained in this work may also be applicable to the similar systems including the biological building blocks as the intra- or intermolecular hydrogen bonding is ubiquitous in the biological environments.

EXPERIMENTAL AND COMPUTATIONAL METHODS

The details of the experimental setup had been given elsewhere.[48,50] The narrow-band picosecond laser pulses ($\Delta E \sim 20$ cm^{-1}, $\Delta t \sim 1.7$ ps) for the pump and probe were generated using two independent tunable optical parametric amplifier (OPA) units. Both OPAs were pumped using the fundamental output (791 nm, 1 kHz) of a picosecond Ti:sapphire regenerative amplifier system, which is seeded by a mode-locked femtosecond Ti:sapphire oscillator at the repetition rate of 80 MHz. The picosecond pump and probe pulses were attenuated using several ND filters and colinearly aligned into a high-vacuum chamber (10^{-8} Torr) through a CaF_2 window without using focusing lens. The angle of the polarization axes between pump and probe pulses was kept at 54.7° during the measurement. The pump−probe time delay was manipulated using a 300 mm-long mechanical translational stage combined with a hallow retroreflector. The samples of chlorine-substituted phenols and thiophenols were seeded in the helium buffer gas with a backing pressure of 3 bar and supersonically expanded into the vacuum chamber using a pulsed Even-Lavie valve through a 150 μm-diameter nozzle orifice at the repetition rate of 20 Hz. The molecular beam collimated by a 1 mm diameter skimmer was crossed by the picosecond pulses in the ion extraction region, and the resultant parent or fragment ions were then detected by a mass-gated time-of-flight (TOF) microchannel plate (MCP) detector. The ion signals were digitized by an oscilloscope and recorded as a function of pump−probe time delay for the analysis. The minimum energy geometries of the title molecules in the ground electronic state (S_0) have been optimized using density functional theory (DFT) with the CAM-B3LYP functional, second order coupled cluster model with the resolution of the identity approximation (RICC2), or complete active space self-consistent field (CASSCF) method. For the adiabatic potential energy curves along the internal conversion reaction coordinate, single point energy calculations were carried out using the CASPT2 level of theory at the DFT-relaxed S_1 geometries while scanning the C−Cl bond length. The active space employed for the CASSCF calculations was comprised of 10 electrons and 10 orbitals, three pairs of Hückel-type π/π^* orbitals, σ_{CCl} and σ_{CCl}^*, and nonbonding *p*-orbitals on oxygen and chlorine. The CASPT2 calculations were performed with an imaginary level shift of 0.4 au. All *ab initio* calculations were carried out using Gaussian (version 09),[87] Molpro (version 2010.1),[88] or Turbomole (version 7.0.2)[89] software suites.

ASSOCIATED CONTENT

Supporting Information

The Supporting Information is available free of charge at https://pubs.acs.org/doi/10.1021/acs.jpclett.3c02208.

R2PI spectra and time-resolved ion transients of title molecules, H or D atom action spectra of 2-chlorophenol, and calculated equilibrium geometries of title molecules in the S_1 state (PDF)

AUTHOR INFORMATION

Corresponding Author

Sang Kyu Kim − *Department of Chemistry, KAIST, Daejeon 34141, Republic of Korea;* orcid.org/0000-0003-4803-1327; Email: sangkyukim@kaist.ac.kr

https://doi.org/10.1021/acs.jpclett.3c02208
J. Phys. Chem. Lett. 2023, 14, 8428−8436

Authors

Junggil Kim − *Department of Chemistry, KAIST, Daejeon 34141, Republic of Korea*

Kyung Chul Woo − *Department of Chemistry, KAIST, Daejeon 34141, Republic of Korea;* Present Address: Sandia National Laboratory, 7011 East Ave, Livermore, CA 94550, United States; orcid.org/0000-0002-9387-9397

Minseok Kang − *Department of Chemistry, KAIST, Daejeon 34141, Republic of Korea*

Complete contact information is available at: https://pubs.acs.org/10.1021/acs.jpclett.3c02208

Notes

The authors declare no competing financial interest.

■ ACKNOWLEDGMENTS

This work was financially supported by the National Research Foundation (NRF) of Korea under the projects 2019R1A6A1A10073887 and RS-2023-00208926. This work was also partially supported by the Technology Innovation Program Development Program (20016007) funded by the Ministry of Trade, Industry & Energy (MOTIE, Korea).

■ REFERENCES

(1) Sobolewski, A. L.; Domcke, W.; Dedonder-Lardeux, C.; Jouvet, C. Excited-state hydrogen detachment and hydrogen transfer driven by repulsive $^1\pi\sigma^*$ states: A new paradigm for nonradiative decay in aromatic biomolecules. *Phys. Chem. Chem. Phys.* **2002**, *4*, 1093−1100.

(2) Ashfold, M. N. R.; King, G. A.; Murdock, D.; Nix, M. G. D.; Oliver, T. A. A.; Sage, A. G. $\pi\sigma^*$ excited states in molecular photochemistry. *Phys. Chem. Chem. Phys.* **2010**, *12*, 1218−1238.

(3) Roberts, G. M.; Stavros, V. G. The role of $\pi\sigma^*$ states in the photochemistry of heteroaromatic biomolecules and their subunits: Insights from gas-phase femtosecond spectroscopy. *Chem. Sci.* **2014**, *5*, 1698−1722.

(4) You, H. S.; Han, S.; Yoon, J.-H.; Lim, J. S.; Lee, J.; Kim, S.-Y.; Ahn, D.-S.; Lim, J. S.; Kim, S. K. Structure and dynamic role of conical intersections in the $\pi\sigma^*$-mediated photodissociation reactions. *Int. Rev. Phys. Chem.* **2015**, *34*, 429−459.

(5) Kim, J.; Woo, K. C.; Kim, K. K.; Kang, M.; Kim, S. K. Tunneling dynamics dictated by the multidimensional conical intersection seam in the $\pi\sigma^*$-mediated photochemistry of heteroaromatic molecules. *Bull. Korean Chem. Soc.* **2022**, *43*, 150−164.

(6) Schoenlein, R. W.; Peteanu, L. A.; Mathies, R. A.; Shank, C. V. The first step in vision: Femtosecond isomerization of rhodopsin. *Science* **1991**, *254*, 412−415.

(7) Satzger, H.; Townsend, D.; Zgierski, M. Z.; Patchkovskii, S.; Ullrich, S.; Stolow, A. Primary processes underlying the photostability of isolated DNA bases: Adenine. *Proc. Natl. Acad. Sci. U.S.A.* **2006**, *103*, 10196−10201.

(8) Asturiol, D.; Lasorne, B.; Worth, G. A.; Robb, M. A.; Blancafort, L. Exploring the sloped-to-peaked S_2/S_1 seam of intersection of thymine with electronic structure and direct quantum dynamics calculations. *Phys. Chem. Chem. Phys.* **2010**, *12*, 4949−4958.

(9) Soorkia, S.; Jouvet, C.; Grégoire, G. UV photoinduced dynamics of conformer-resolved aromatic peptides. *Chem. Rev.* **2020**, *120*, 3296−3327.

(10) Jouvet, C.; Miyazaki, M.; Fujii, M. Revealing the role of excited state proton transfer (ESPT) in excited state hydrogen transfer (ESHT): Systematic study in phenol-$(NH_3)_n$ clusters. *Chem. Sci.* **2021**, *12*, 3836−3856.

(11) Yarkony, D. R. Conical intersections: Diabolical and often misunderstood. *Acc. Chem. Res.* **1998**, *31*, 511−518.

(12) Yarkony, D. R. Nuclear dynamics near conical intersections in the adiabatic representation: I. The effects of local topography on interstate transitions. *J. Chem. Phys.* **2001**, *114*, 2601−2613.

(13) Tully, J. C. Perspective: Nonadiabatic dynamics theory. *J. Chem. Phys.* **2012**, *137*, 22A301.

(14) Malhado, J. P.; Bearpark, M. J.; Hynes, J. T. Non-adiabatic dynamics close to conical intersections and the surface hopping perspective. *Front. Chem.* **2014**, *2*, 97.

(15) Ashfold, M. N. R.; Kim, S. K. Non-Born-Oppenheimer effects in molecular photochemistry: An experimental perspective. *Philos. Trans. R. Soc. A* **2022**, *380*, 20200376.

(16) Herzberg, G.; Longuet-Higgins, H. C. Intersection of potential energy surfaces in polyatomic molecules. *Discuss. Faraday Soc.* **1963**, *35*, 77−82.

(17) Herzberg, G. *Electronic Spectra and Electronic Structure of Polyatomic Molecules*; Van Nostrand: New York, 1966.

(18) Schinke, R. *Photodissociation Dynamics: Spectroscopy and Fragmentation of Small Polyatomic Molecules*; Cambridge University Press, Cambridge, U.K., 1993.

(19) Lim, J. S.; Kim, S. K. Experimental probing of conical intersection dynamics in the photodissociation of thioanisole. *Nat. Chem.* **2010**, *2*, 627−632.

(20) Roberts, G. M.; Hadden, D. J.; Bergendahl, L. T.; Wenge, A. M.; Harris, S. J.; Karsili, T. N. V.; Ashfold, M. N. R.; Paterson, M. J.; Stavros, V. G. Exploring quantum phenomena and vibrational control in σ^* mediated photochemistry. *Chem. Sci.* **2013**, *4*, 993−1001.

(21) Han, S.; Lim, J. S.; Yoon, J.-H.; Lee, J.; Kim, S.-Y.; Kim, S. K. Conical intersection seam and bound resonances embedded in continuum observed in the photodissociation of thioanisole-d_3. *J. Chem. Phys.* **2014**, *140*, 054307.

(22) Woo, K. C.; Kang, D. H.; Kim, S. K. Real-time observation of nonadiabatic bifurcation dynamics at a conical intersection. *J. Am. Chem. Soc.* **2017**, *139*, 17152−17158.

(23) Li, S. L.; Truhlar, D. G. Full-dimensional multi-state simulation of the photodissociation of thioanisole. *J. Chem. Phys.* **2017**, *147*, 044311.

(24) Lim, J. S.; You, H. S.; Kim, S.-Y.; Kim, S. K. Experimental observation of nonadiabatic bifurcation dynamics at resonances in the continuum. *Chem. Sci.* **2019**, *10*, 2404−2412.

(25) Lee, H.; Kim, S.-Y.; Kim, S. K. Multidimensional characterization of the conical intersection seam in the normal mode space. *Chem. Sci.* **2020**, *11*, 6856−6861.

(26) Li, C.; Hou, S.; Wang, Z.; Xie, C. Nonadiabatic heavy atom tunneling in $^1n\sigma^*$-mediated photodissociation of thioanisole. *Phys. Chem. Chem. Phys.* **2023**, *25*, 18797−18807.

(27) Nix, M. G. D.; Devine, A. L.; Cronin, B.; Dixon, R. N.; Ashfold, M. N. R. High resolution photofragment translational spectroscopy studies of the near ultraviolet photolysis of phenol. *J. Chem. Phys.* **2006**, *125*, 133318.

(28) Nix, M. G. D.; Devine, A. L.; Dixon, R. N.; Ashfold, M. N. R. Observation of geometric phase effect induced photodissociation dynamics in phenol. *Chem. Phys. Lett.* **2008**, *463*, 305−308.

(29) Roberts, G. M.; Chatterley, A. S.; Young, J. D.; Stavros, V. G. Direct observation of hydrogen tunneling dynamics in photoexcited phenol. *J. Phys. Chem. Lett.* **2012**, *3*, 348−352.

(30) Xie, C.; Ma, J.; Zhu, X.; Yarkony, D. R.; Xie, D.; Guo, H. Nonadiabatic tunneling in photodissociation of phenol. *J. Am. Chem. Soc.* **2016**, *138*, 7828−7831.

(31) King, G. A.; Oliver, T. A. A.; Nix, M. G. D.; Ashfold, M. N. R. High resolution photofragment translational spectroscopy studies of the ultraviolet photolysis of phenol-d_5. *J. Phys. Chem. A* **2009**, *113*, 7984−7993.

(32) Lai, H. Y.; Jhang, W. R.; Tseng, C.-M. Communication: Mode-dependent excited-state lifetime of phenol under the S_1/S_2 conical intersection. *J. Chem. Phys.* **2018**, *149*, 031104.

(33) Woo, K. C.; Kim, S. K. Multidimensional H atom tunneling dynamics of phenol: Interplay between vibrations and tunneling. *J. Phys. Chem. A* **2019**, *123*, 1529−1537.

(34) Kim, J.; Woo, K. C.; Kim, S. K. Mode-dependent H atom tunneling dynamics of the S_1 phenol is resolved by the simple topographic view of the potential energy surfaces along the conical intersection seam. *J. Chem. Phys.* **2023**, *158*, 104301.

(35) Devine, A. L.; Nix, M. G. D.; Cronin, B.; Ashfold, M. N. R. Near-UV photolysis of substituted phenols, I: 4-fluoro-, 4-chloro- and 4-bromophenol. *Phys. Chem. Chem. Phys.* **2007**, *9*, 3749−3762.
(36) King, G. A.; Devine, A. L.; Nix, M. G. D.; Kelly, D. E.; Ashfold, M. N. R. Near-UV photolysis of substituted phenols: Part II. 4-, 3-, and 2-methylphenol. *Phys. Chem. Chem. Phys.* **2008**, *10*, 6417−6429.
(37) Pino, G. A.; Oldani, A. N.; Marceca, E.; Fujii, M.; Ishiuchi, S.-I.; Miyazaki, M.; Broquier, M.; Dedonder, C.; Jouvet, C. Excited state hydrogen transfer dynamics in substituted phenols and their complexes with ammonia: $\pi\pi^*$-$\pi\sigma^*$ energy gap propensity and *ortho*-substitution effect. *J. Chem. Phys.* **2010**, *133*, 124313.
(38) King, G. A.; Oliver, T. A. A.; Dixon, R. N.; Ashfold, M. N. R. Vibrational energy redistribution in catechol during ultraviolet photolysis. *Phys. Chem. Chem. Phys.* **2012**, *14*, 3338−3345.
(39) Weiler, M.; Miyazaki, M.; Féraud, G.; Ishiuchi, S.-I.; Dedonder, C.; Jouvet, C.; Fujii, M. Unusual behavior in the first excited state lifetime of catechol. *J. Phys. Chem. Lett.* **2013**, *4*, 3819−3823.
(40) Capello, M. C.; Broquier, M.; Ishiuchi, S.-I.; Sohn, W. Y.; Fujii, M.; Dedonder-Lardeux, C.; Jouvet, C.; Pino, G. A. Fast nonradiative decay in *o*-aminophenol. *J. Phys. Chem. A* **2014**, *118*, 2056−2062.
(41) Soorkia, S.; Broquier, M.; Grégoire, G. Conformer- and mode-specific excited state lifetimes of cold protonated tyrosine ions. *J. Phys. Chem. Lett.* **2014**, *5*, 4349−4355.
(42) Karsili, T. N. V.; Wenge, A. M.; Marchetti, B.; Ashfold, M. N. R. Symmetry matters: Photodissociation dynamics of symmetrically *versus* asymmetrically substituted phenols. *Phys. Chem. Chem. Phys.* **2014**, *16*, 588−598.
(43) Woo, K. C.; Kim, J.; Kim, S. K. Conformer-specific tunneling dynamics dictated by the seam coordinate of the conical intersection. *J. Phys. Chem. Lett.* **2021**, *12*, 1854−1861.
(44) Kim, K. K.; Kim, J.; Woo, K. C.; Kim, S. K. S_1-state decay dynamics of benzenediols (catechol, resorcinol, and hydroquinone) and their 1:1 water clusters. *J. Phys. Chem. A* **2021**, *125*, 7655−7661.
(45) Devine, A. L.; Nix, M. G. D.; Dixon, R. N.; Ashfold, M. N. R. Near-ultraviolet photodissociation of thiophenol. *J. Phys. Chem. A* **2008**, *112*, 9563−9574.
(46) You, H. S.; Han, S.; Lim, J. S.; Kim, S. K. ($\pi\pi^*/\pi\sigma^*$) conical intersection seam experimentally observed in the S-D bond dissociation reaction of thiophenol-d_1. *J. Phys. Chem. Lett.* **2015**, *6*, 3202−3208.
(47) Han, S.; You, H. S.; Kim, S.-Y.; Kim, S. K. Dynamic role of the intramolecular hydrogen bonding in nonadiabatic chemistry revealed in the UV photodissociation reactions of 2-fluorothiophenol and 2-chlorothiophenol. *J. Phys. Chem. A* **2014**, *118*, 6940−6949.
(48) Lim, J. S.; You, H. S.; Kim, S.-Y.; Kim, J.; Park, Y. C.; Kim, S. K. Vibronic structure and predissociation dynamics of 2-methoxythiophenol (S_1): The effect of intramolecular hydrogen bonding on nonadiabatic dynamics. *J. Chem. Phys.* **2019**, *151*, 244305.
(49) Woo, K. C.; Kim, S. K. Real-time tunneling dynamics through adiabatic potential energy surfaces shaped by a conical intersection. *J. Phys. Chem. Lett.* **2020**, *11*, 6730−6736.
(50) Kim, J.; Woo, K. C.; Kim, K. K.; Kim, S. K. $\pi\sigma^*$-mediated nonadiabatic tunneling dynamics of thiophenols in S_1: The semi-classical approaches. *J. Phys. Chem. A* **2022**, *126*, 9594−9604.
(51) Lipert, R. J.; Bermudez, G.; Colson, S. D. Pathways of S_1 decay in phenol, indoles, and water complexes of phenol and indole in a free jet expansion. *J. Phys. Chem.* **1988**, *92*, 3801−3805.
(52) Young, J. D.; Staniforth, M.; Chatterley, A. S.; Paterson, M. J.; Roberts, G. M.; Stavros, V. G. Relaxation dynamics of photoexcited resorcinol: Internal conversion *versus* H atom tunneling. *Phys. Chem. Chem. Phys.* **2014**, *16*, 550−562.
(53) Yamamoto, S.; Ebata, T.; Ito, M. Rotational isomers of *o*-chlorophenol and their different emission properties. *J. Phys. Chem.* **1989**, *93*, 6340−6345.
(54) Harris, S. J.; Karsili, T. N. V.; Murdock, D.; Oliver, T. A. A.; Wenge, A. M.; Zaouris, D. K.; Ashfold, M. N. R.; Harvey, J. N.; Few, J. D.; Gowrie, S.; Hancock, G.; Hadden, D. J.; Roberts, G. M.; Stavros, V. G.; Spighi, G.; Poisson, L.; Soep, B. A multipronged comparative study of the ultraviolet photochemistry of 2-, 3-, and 4-chlorophenol in the gas phase. *J. Phys. Chem. A* **2015**, *119*, 6045−6056.
(55) Allan, E. A.; Reeves, L. W. The use of the chemical shift parameter for study of intramolecular hydrogen bonds. *J. Phys. Chem.* **1962**, *66*, 613−617.
(56) Carlson, G. L.; Fateley, W. G.; Manocha, A. S.; Bentley, F. F. Torsional frequencies and enthalpies of intramolecular hydrogen bonds of *o*-halophenols. *J. Phys. Chem.* **1972**, *76*, 1553−1557.
(57) Shin, D. N.; Hahn, J. W.; Jung, K.-H.; Ha, T.-K. Study of the *cis* and *trans* conformers of 2-halophenols using coherent anti-Stokes Raman spectroscopic and quantum chemical methods. *J. Raman Spectrosc.* **1998**, *29*, 245−249.
(58) Akai, N.; Kudoh, S.; Takayanagi, M.; Nakata, M. Photoreaction mechanisms of 2-chlorophenol and its multiple chloro-substituted derivatives studied by low-temperature matrix-isolation infrared spectroscopy and density-functional-theory calculations. *J. Photochem. Photobiol., A* **2001**, *146*, 49−57.
(59) Hirokawa, S.; Imasaka, T.; Imasaka, T. S_0 and S_1 states of monochlorophenols: Ab initio CASSCF MO study. *J. Phys. Chem. A* **2001**, *105*, 9252−9257.
(60) Ahn, D.-S.; Park, S.-W.; Lee, S.; Kim, B. Effects of substituting group on the hydrogen bonding in phenol-H_2O complexes: Ab initio study. *J. Phys. Chem. A* **2003**, *107*, 131−139.
(61) Uchimura, T.; Hafner, K.; Zimmermann, R.; Imasaka, T. Multiphoton ionization mass spectrometry of chlorophenols as indicators for dioxins. *Appl. Spectrosc.* **2003**, *57*, 461−465.
(62) Zhao, G.-J.; Han, K.-L. Hydrogen bonding in the electronic excited state. *Acc. Chem. Res.* **2012**, *45*, 404−413.
(63) Tuna, D.; Sobolewski, A. L.; Domcke, W. Mechanisms of ultrafast excited-state deactivation in adenosine. *J. Phys. Chem. A* **2014**, *118*, 122−127.
(64) Kim, J.; Lim, J. S.; Noh, H.-R.; Kim, S. K. Experimental observation of the Autler-Townes splitting in polyatomic molecules. *J. Phys. Chem. Lett.* **2020**, *11*, 6791−6795.
(65) Lin, G.-S.-M.; Xie, C.; Xie, D. Three-dimensional diabatic potential energy surfaces for the photodissociation of thiophenol. *J. Phys. Chem. A* **2017**, *121*, 8432−8439.
(66) Zhang, L.; Truhlar, D. G.; Sun, S. Electronic spectrum and characterization of diabatic potential energy surfaces for thiophenol. *Phys. Chem. Chem. Phys.* **2018**, *20*, 28144−28154.
(67) Blaser, S.; Trachsel, M. A.; Lobsiger, S.; Wiedmer, T.; Frey, H.-M.; Leutwyler, S. Gas-phase cytosine and cytosine-N_1-derivatives have 0.1 - 1 ns lifetimes near the S_1 state minimum. *J. Phys. Chem. Lett.* **2016**, *7*, 752−757.
(68) Trachsel, M. A.; Blaser, S.; Lobsiger, S.; Siffert, L.; Frey, H.-M.; Blancafort, L.; Leutwyler, S. Locating cytosine conical intersections by laser experiments and *ab initio* calculations. *J. Phys. Chem. Lett.* **2020**, *11*, 3203−3210.
(69) Lipert, R. J.; Colson, S. D. Deuterium isotope effects on S_1 radiationless decay in phenol and on intermolecular vibrations in the phenol-water complex. *J. Phys. Chem.* **1989**, *93*, 135−139.
(70) Ratzer, C.; Küpper, J.; Spangenberg, D.; Schmitt, M. The structure of phenol in the S_1-state determined by high resolution UV-spectroscopy. *Chem. Phys.* **2002**, *283*, 153−169.
(71) Kadi, M.; Davidsson, J.; Tarnovsky, A. N.; Rasmusson, M.; Åkesson, E. Photodissociation of aryl halides in the gas phase studied with femtosecond pump-probe spectroscopy. *Chem. Phys. Lett.* **2001**, *350*, 93−98.
(72) Deguchi, T.; Takeyasu, N.; Imasaka, T. Measurement of the first-excited-singlet-state lifetime of chlorobenzenes by a pump-probe method using a narrow-band tunable picosecond laser. *Apple. Spectrosc.* **2002**, *56*, 1241−1243.
(73) Anders Borg, O.; Karlsson, D.; Isomäki-Krondahl, M.; Davidsson, J.; Lunell, S. Predissociation of chlorobenzene, beyond the pseudo-diatomic model. *Chem. Phys. Lett.* **2008**, *456*, 123−126.
(74) Liu, B.; Wang, B.; Wang, Y.; Wang, L. Ultrafast dynamics of chlorobenzene clusters. *Chem. Phys. Lett.* **2009**, *477*, 266−270.

https://doi.org/10.1021/acs.jpclett.3c02208
J. Phys. Chem. Lett. 2023, 14, 8428−8436

(75) Liu, Y.-Z.; Qin, C.-C.; Zhang, S.; Wang, Y.-M.; Zhang, B. Ultrafast dynamics of the first excited state of chlorobenzene. *Acta Phys. -Chim. Sin.* **2011**, *27*, 965−970.
(76) Zheng, Q.; Qin, C.; Long, J.; Tang, B.; Zhang, S.; Zhang, B. Ultrafast dynamics of o-fluorophenol studied with femtosecond time-resolved photoelectron and photoion spectroscopy. *Sci. China Mech. Astron.* **2010**, *53*, 1040−1044.
(77) Deng, X.; Tang, Y.; Song, X.; Liu, K.; Gu, Z.; Zhang, B. Photolysis dynamics of m- and o-fluorophenol: Substitution effects on tunneling mechanism. *Chemosphere* **2020**, *253*, 126747.
(78) Salman, S. R.; Kudier, A. R. ^{1}H NMR study of dilution and complex formation of *o*-halophenols. *Spectrochim. Acta, Part A* **1990**, *46*, 1147−1152.
(79) Simperler, A.; Lampert, H.; Mikenda, W. Intramolecular interactions in ortho-substituted phenols: Survey of DFT-B3LYP calculated data. *J. Mol. Struct.* **1998**, *448*, 191−199.
(80) John, U.; Kuriakose, S.; Nair, K. P. R. Vibrational overtone spectra of *o*-fluorophenol and the ″anomalous″ order of intramolecular hydrogen bonding strengths. *Spectrochim. Acta, Part A* **2007**, *68*, 331−336.
(81) Abraham, M. H.; Abraham, R. J.; Aliev, A. E.; Tormena, C. F. Is there an intramolecular hydrogen bond in 2-halophenol? A theoretical and spectroscopic investigation. *Phys. Chem. Chem. Phys.* **2015**, *17*, 25151−25159.
(82) Zeoly, L. A.; Coelho, F.; Cormanich, R. A. Intramolecular H-bond is formed in 2-fluorophenol and 2-fluorothiophenol, but it may not be the main pathway of the J_{FH} coupling constant transmission. *J. Phys. Chem. A* **2019**, *123*, 10072−10078.
(83) Rosenberg, R. E.; Chapman, B. K.; Ferrill, R. N.; Jung, E. S.; Samaan, C. A. Approximating the strength of the intramolecular hydrogen bond in 2-fluorophenol and related compounds: A new application of a classic technique. *J. Phys. Chem. A* **2020**, *124*, 3851−3858.
(84) Lim, J. S. *Spectroscopy and Photodissociation Dynamics on Nonplanar Excited State of Ortho-Substituted Thiophenol and Thioanisole*. Ph.D. Dissertation; KAIST, Republic of Korea: 2018.
(85) Lim, J. S.; You, H. S.; Han, S.; Kim, S. K. Photodissociation dynamics of ortho-substituted thiophenols at 243 nm. *J. Phys. Chem. A* **2019**, *123*, 2634−2639.
(86) Hayashi, M.; Ichihara, R.; Akai, N.; Nakata, M. Photoreaction of 2-chlorothiophenol studied by low-temperature matrix-isolation IR spectroscopy with DFT calculation. *J. Mol. Struct.* **2021**, *1244*, 130909.
(87) Frisch, M. J.; Trucks, G. W.; Schlegel, H. B.; Scuseria, G. E.; Robb, M. A.; Cheeseman, J. R.; Scalmani, G.; Barone, V.; Mennucci, B.; Petersson, G. A.; Nakatsuji, H.; Caricato, M.; Li, X.; Hratchian, H. P.; Izmaylov, A. F.; Bloino, J.; Zheng, G.; Sonnenberg, J. L.; Hada, M.; Ehara, M.; Toyota, K.; Fukuda, R.; Hasegawa, J.; Ishida, M.; Nakajima, T.; Honda, Y.; Kitao, O.; Nakai, H.; Vreven, T.; Montgomery, Jr., J. A.; Peralta, J. E.; Ogliaro, F.; Bearpark, M.; Heyd, J. J.; Brothers, E.; Kudin, K. N.; Staroverov, V. N.; Kobayashi, R.; Normand, J.; Raghavachari, K.; Rendell, A.; Burant, J. C.; Iyengar, S. S.; Tomasi, J.; Cossi, M.; Rega, N.; Millam, J. M.; Klene, M.; Knox, J. E.; Cross, J. B.; Bakken, V.; Adamo, C.; Jaramillo, J.; Gomperts, R.; Stratmann, R. E.; Yazyev, O.; Austin, A. J.; Cammi, R.; Pomelli, C.; Ochterski, J. W.; Martin, R. L.; Morokuma, K.; Zakrzewski, V. G.; Voth, G. A.; Salvador, P.; Dannenberg, J. J.; Dapprich, S.; Daniels, A. D.; Farkas, Ö.; Foresman, J. B.; Ortiz, J. V.; Cioslowski, J.; Fox, D. J. *Gaussian 09*, Rev. D.1; Gaussian Inc.: Wallingford, CT, 2009.
(88) Werner, H.-J.; Knowles, P. J.; Knizia, G.; Manby, F. R.; Schütz, M. Molpro: A general-purpose quantum chemistry program package. *Wiley Interdiscip. Rev.: Comput. Mol. Sci.* **2012**, *2*, 242−253.
(89) *TURBOMOLE V7.0.2 2015*; a development of University of Karlsruhe and Forschungszentrum Karlsruhe GmbH, 1989−2007, TURBOMOLE GmbH, since 2007; available from http://www.turbomole.org (accessed August 6, 2023).

https://doi.org/10.1021/acs.jpclett.3c02208
J. Phys. Chem. Lett. 2023, 14, 8428−8436